AD-A259 917

DEFENSIO PER SCIENTIAM

SUPPRESSION OF
POWER LINE HARMONIC INTERFERENCE
IN HF SURFACE-WAVE RADAR (U)

by

Hank Leong

DTIC
SELECTE
FEB 0 4 1993
S
B
D

404570

93-02022
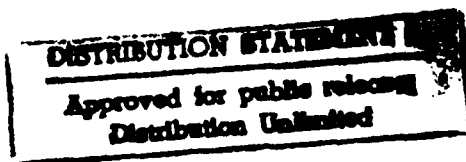
3138

DEFENCE RESEARCH ESTABLISHMENT OTTAWA
REPORT N0. 1137

Canada

October 1992
Ottawa

93 2 3 036

SUPPRESSION OF
POWER LINE HARMONIC INTERFERENCE
IN HF SURFACE-WAVE RADAR (U)

by

Hank Leong
Surface Radar Section
Radar Division

DEFENCE RESEARCH ESTABLISHMENT OTTAWA
REPORT NO. 1137

Abstract

Experimental data of the Cape Bonavista High-Frequency Surface-Wave Radar (HFSWR) facility was contaminated by power line harmonics. The harmonics modulate the radar signal (mainly sea clutter) and replicate it into the Doppler spectrum. The spectral replicas distort the noise and sea clutter statistics in the signal. It is necessary to suppress them before the statistics can be obtained.

A new process based on optimizations is presented for suppressing the interference. This process minimizes the spectral power of the sea clutter with respect to the amplitudes and phases of the harmonics. It is capable of removing the spectral replicas without adversely altering the statistics. This process, however, requires adequate modelling of the harmonics. A large number of parameters are required because the harmonics may have a fluctuating fundamental frequency and fluctuating amplitudes. Therefore the process can be numerically complex. To implement our process, one must use approximations in the signal model. If the amplitudes and the fundamental frequency are approximated with constants, the process can still be effective for a short HFSWR data series. For some 256-point data series, more than 20 dB of the peak interference can be reduced. For a long HFSWR data series, the same process can be applied by first dividing it into several short data segments, and then optimizing on the individual segments. With this slightly revised approach, up to 20 dB of the peak interference can be suppressed for a long data series.

The process does not account for any anomalies in the HFSWR data. The data may sometimes have (i) large noise spikes, (ii) unequal strengths of interference in I and Q channels, and (iii) irregular waveform patterns. If these anomalies exist, the process becomes less effective.

iii

Résumé

Les données expérimentales concernant le radar de surface à haute fréquence prises aux installations de Cape Bonavista étaient contaminées par des harmoniques provenant de l'alimentation. Ces harmoniques modulent le signal radar (principalement du fouillis de mer) et le répète dans le spectre Doppler. Puisque les répliques spectrales distordent les statistiques du bruit et du fouillis de mer dans le signal, il est donc nécessaire de les éliminer avant d'obtenir ces statistiques.

Ce rapport présente une nouvelle méthode, basée sur des optimisations, qui minimise la puissance spectrale du fouillis de mer relativement à l'amplitude et à la phase des harmoniques. Cette méthode élimine les répliques spectrales sans altérer trop sévèrement les statistiques du bruit et du fouillis de mer. Elle requiert cependant une modélisation adéquate des harmoniques. Cette modélisation utilise un grand nombre de paramètres parce que les harmoniques peuvent avoir une fréquence fondamentale et des amplitudes qui fluctuent, rendant la méthode complexe à évaluer. Il est donc nécessaire d'utiliser certaines approximations dans le modèle du signal pour implémenter notre technique. Par exemple, si les amplitudes et la fréquence fondamentale sont approximées par des constantes, la technique fonctionne pour une courte série de données radar: pour une série de données de 256 points, nous pouvons réduire l'interférence maximale de plus de 20 dB. Cette technique peut aussi être appliquée à une longue série de données en divisant celles-ci en segments plus courts pour ensuite optimiser chaque segment individuellement. Nous réussissons à réduire de 20 dB l'interférence maximale avec cette approche.

Cette méthode ne tient pas compte des anomalies dans les données radar. Ces données peuvent parfois avoir (i) de grandes pointes de bruit, (ii) des diagrammes d'onde irréguliers , (iii) l'interférence peut avoir une puissance différente dans les canaux I et Q. Si ces anomalies existent, la technique devient moins efficace.

Executive Summary

Experimental High-Frequency Surface-Wave Radar (HFSWR) data was collected in the summer of 1989 by NORDCO Limited of Newfoundland under a contract to DND [1]. The data consists of a set of time series of the radar's sea echoes from individual range gates. They are to be used for studying the characteristics of sea clutter, noise and possible targets.

Preliminary analysis of the data revealed that the time series were contaminated by power line harmonics. These harmonics modulate the received radar signal and replicate the radar echo (mainly sea clutter) into four different Doppler frequencies in the power spectrum. The spectral replicas distort noise statistics and impair target detection. It is necessary to suppress them before the noise and sea-clutter statistics can be obtained.

This report presents a new process based on optimizations. In the process, the received radar signal is modelled as sea clutter plus modulation of the sea clutter by the power line harmonics. The spectral power of the sea clutter in the frequency region of the spectral replicas is then minimized with respect to the amplitudes and phases of the harmonics. If the radar signal is modelled adequately, this process is capable of removing the interference of the spectral replicas without adversely altering the noise and sea-clutter statistics in the radar signal.

In the experimental data, however, the fundamental frequency of the harmonics fluctuates at 60 Hz, and consequently the phases of the harmonics are time-dependent. The amplitudes of the harmonics also seem to fluctuate with time. A large number of parameters are required to model the fluctuations. The process can therefore be numerically complex.

To implement the process, one must use approximations in the signal model. If the amplitudes and the fundamental frequency of the harmonics are approximated with constants, the process can still be effective for short data series. For example, for some 256-point data series, more than 20 dB suppression of the peak interference is possible. For a long HFSWR data series, the same process can be applied by first dividing it into several short data segments (e.g., 256 points, or even 128 points), and then optimizing on the individual data segments. With this slightly revised approach, up to 20 dB of the peak interference can be suppressed for ⸱ long HFSWR data series.

The optimization process, however, becomes less effective if there are anomalies in the experimental time series. The possible anomalies include (i) large noise spikes, (ii) unequal strengths of interference in I and Q channels, and (iii) irregular patterns in the time waveform.

Table of Contents

List of Figures

1.0 Introduction

Experimental High-Frequency Surface-Wave Radar (HFSWR) data was collected in the summer of 1989 by NORDCO Limited of Newfoundland under a contract to DND [1]. The HFSWR facility is located in Cape Bonavista, Newfoundland. It employs a 1.95 MHz Loran A transmitter and an 11-element array receiver. The omni-directional transmitter emits trains of 50 μs, raised cosine, pulses at a pulse repetition frequency (PRF) of 25 Hz. The receiver aims offshore from Cape Bonavista. The received signal is sampled and then processed to yield a set of time series of the sea echoes from individual range gates. The effective sampling rate, f_s, of these time series is equal to the PRF, i.e., 25 Hz.

The data normally consists of sea clutter, noise and possible targets, with the sea clutter dominating. However, preliminary analysis of the data indicated that the time series were contaminated by power line harmonics. The harmonics modulate the received radar signal and replicate the signal in the frequency domain at the frequencies of the harmonics. The frequencies of the harmonics, f, are equal to the multiples of their fundamental frequency f_1. If $f_1 = 60$ Hz, then f = +/- m(60 Hz), m=1,2,3, ..., and the spectral replicas of the radar signal would appear at f= +/- m(60 Hz).

The sampling process further replicates the modulated signal at the multiples of the sampling frequency f_s. Since f_s is less than the frequencies of the modulation harmonics, the sampled time series are subject to aliasing [2]. Aliasing causes an overlapping of the sampled spectral replicas. A spectral component located at a frequency f > f_s in the modulated signal would be folded onto a frequency f_a < f_s in the sampled data. The latter frequency f_a is given by

$$f_a = MOD(f, f_s) \tag{1}$$

For the modulation spectral replicas centred at f = +/- m(60 Hz), m=1,2,3, ..., the aliased spectra would appear at one of the following frequencies: -10, -5, 5 and 10 Hz.

Figure 1 shows a power spectral plot of a 1024-point HFSWR time series. We have chosen the frequency range in Figure 1 between 0 and 25 Hz, instead of the normal Doppler range between -12.5 and 12.5 Hz. Consequently, the modulation replicas now appear at 5, 10, 15 and 20 Hz.

1
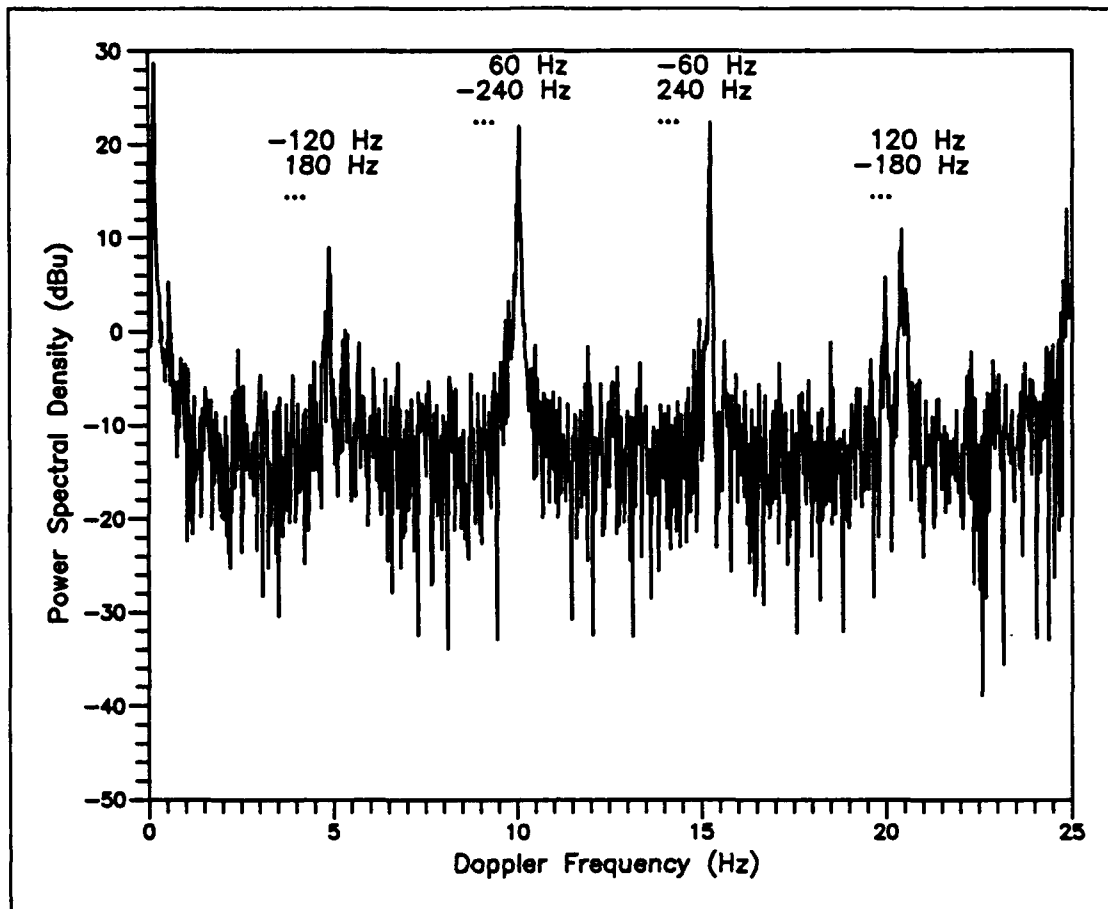
Figure 1   Power Spectrum of a Typical Time Series
in the Cape Bonavista HFSWR Experiment

The objective of analyzing the data is to obtain information on the statistics of noise and sea clutter to determine the proper detection threshold that will yield an acceptable probability of false alarm (P_{fa}). Since most HF radar systems have poor range and azimuthal resolution, this information cannot be obtained spatially across the range gates. Consequently, the noise and sea clutter statistics can only be calculated after Doppler processing of the data, e.g., by conventional Discrete Fourier Transform (DFT).

The spectral spread of the dominant sea clutter is normally confined to the interval between -1 and 1 Hz in the Doppler spectrum, i.e., to the intervals between 0 and 1 Hz, and between 24 and 25 Hz in Figure 1. The noise statistics may therefore be deduced by observing the power spectrum in the interval between 1 and 24 Hz. However, the presence of the spectral replicas at 5, 10, 15 and 20 Hz poses a serious problem because the spectral replicas not only occupy a large portion of the spectrum, but also raise the noise level of the signal. In this report, we explore means of suppressing the interference of these spectral replicas so that all the data in the interval can be available for the determination of the noise and sea clutter statistics.

2

The technique used to suppress the interference must preserve the noise and sea clutter statistics. The commonly used bandstop filtering technique does not meet this requirement because it not only changes the noise and sea clutter statistics, but also removes any possible target Doppler in the frequency regions of interference.

This report presents a new process based on optimizations to suppress the interference. This process models the radar echo as sea clutter, noise and possible targets (to be referred as sea clutter thereafter) plus the interference of the power line harmonic modulations. It then minimizes the spectral power of the sea clutter in the frequency region of interference with respect to amplitudes and phases of the harmonics. Finally it removes the interference from the sea clutter.

The organization of the report is as follows. In Section 2, the process is formulated with a general signal model: the amplitudes and phases of the harmonics are modelled as polynomial functions of time. A large number of parameters may be required in this signal model, and therefore the process can be numerically complex. In Section 3, the process is then simplified with varying degrees of approximations in the signal model. The results of the process based on the approximations are presented, and the effectiveness of the process is discussed. Finally conclusions and recommendations are presented in Section 4.

2.0 Theoretical Formulation

2.1 Signal Model

The received HFSWR signal, x(t), is modelled as follows:

$$x(t) = c(t)[1+i(t)] \tag{2}$$

where i(t) is the harmonic interference from the power line, and
c(t) is the composite signal of sea clutter, noise and possible targets.

If M is the maximum harmonic number of the interference harmonics, then the signal model can be further expressed as

$$x(t) = c(t)\left(\sum_{m=-M}^{m=M} A_m(t) e^{j[2\pi m f_0 t + \phi_m(t)]}\right) \tag{3}$$

where $A_m(t)$ and $\phi_m(t)$ are the amplitude and phase of the m-th harmonic, $A_0=1$, $\phi_0=0$, and $f_0=60Hz$. We assume that $A_m(t)$ and $\phi_m(t)$ are slow-varying functions of time which can be approximated adequately by polynomials.

$$A_m(t) = a_{m0} + a_{m1}t + a_{m2}t^2 + \ldots$$
$$\phi_m(t) = b_{m0} + b_{m1}t + b_{m2}t^2 + \ldots \tag{4}$$

3

By definition, the fundamental frequency of the harmonic interference is given by

$$f_1(t) = 60 + \frac{1}{2\pi}\frac{d\phi_1(t)}{dt} \qquad (5)$$

We further assume that the time variations in the phases of the harmonics are due to the fluctuations of their frequencies, and that the frequency of the m-th harmonic is equal to the fundamental frequency multiplied by its harmonic number. This implies that the time variations in the phases are due entirely to the fluctuation of the fundamental frequency. Mathematically, if $f_m = mf_1$, then

$$\frac{d\phi_m}{dt} = m\frac{d\phi_1}{dt} \qquad (6)$$

Hence, only the constant term b_{m0} in $\phi_m(t)$ is the signature term for the phase of the m-th harmonic, and all the other terms in $\phi_m(t)$ can be obtained from $\phi_1(t)$, i.e., for p = 1, 2, 3, ...,

$$b_{mp} = m\, b_{1p} \qquad (7)$$

A time series $\{x_n, n=0, 1, 2, ..., N-1\}$ is formed by sampling $x(t)$ at $t=n\Delta t$, where Δt is the sampling period of 1/25 seconds. If T_d is the radar's dwell time, then $N=T_d/\Delta t$. Let c_n denote $c(n\Delta t)$, then

$$x_n = c_n \left(\sum_{m=-M}^{m=M} A_m(n\,\Delta t)\, e^{j[2\pi m f_0\, n\,\Delta t + \phi_m(n\,\Delta t)]} \right) \qquad (8)$$

2.2   Interference Suppression via Optimization

The time series $\{c_n, n=0, 1, 2, ..., N-1\}$ can be obtained from (8) if the amplitudes and phases of the harmonics are known.

$$c_n = \frac{x_n}{\displaystyle\sum_{m=-M}^{m=M} A_m(n\,\Delta t)\, e^{j(2\pi m\, f_0\, n\,\Delta t + \phi_m(n\,\Delta t))}} \qquad (9)$$

4

One way to obtain the amplitudes and phases is to optimize the spectral power of the time series $\{c_n,\ n=0,\ 1,\ 2,\ ...,\ N\text{-}1\}$ in the frequency region of interference, i.e., in the frequency interval encompassing 5, 10, 15 and 20 Hz. This spectral power should be at its minimum when the time series contains no interference. If the frequency interval is between k_1 and k_2, then the spectral power, E, is

$$E = \sum_{k=k_1}^{k_2} |C_k|^2 \qquad (10)$$

where C_k, k=0, 1, 2, ..., N-1, is the DFT of c_n, defined by

$$C_k = \frac{1}{N}\sum_{n=0}^{N-1} c_n e^{-j\frac{2\pi kn}{N}} \qquad (11)$$

Substituting (9) into (11), we have

$$C_k = \frac{1}{N}\sum_{n=0}^{N-1} \left(\frac{x_n e^{-j\frac{2\pi kn}{N}}}{\sum_{m=-M}^{m=M} A_m(n\,\Delta t)\, e^{j(2\pi\, m\, f_0 n\, \Delta t + \phi_m(n\,\Delta t))}} \right) \qquad (12)$$

The necessary conditions for E to be minimized are:

$$\frac{\partial E}{\partial a_{Lp}} = 0$$
$$\frac{\partial E}{\partial b_{Lp}} = 0 \qquad (13)$$

for p=0, 1, 2, ..., and L=-M, -(M-1), ...,-2, -1, 1, 2, ..., M, where L≠0.

Substituting (10) into (13) gives

$$\frac{\partial E}{\partial a_{Lp}} = \sum_{k=k_1}^{k_2} \left(C_k^* \frac{\partial C_k}{\partial a_{Lp}} + C_k \frac{\partial C_k^*}{\partial a_{Lp}} \right) = 0$$
$$\frac{\partial E}{\partial b_{Lp}} = \sum_{k=k_1}^{k_2} \left(C_k^* \frac{\partial C_k}{\partial b_{Lp}} + C_k \frac{\partial C_k^*}{\partial b_{Lp}} \right) = 0 \qquad (14)$$

5

These equations can be further simplified to

$$\sum_{k=k_1}^{k_2}\left(\Re\left(C_k^{\cdot}\frac{\partial C_k}{\partial a_{Lp}}\right)\right) = 0$$

$$\sum_{k=k_1}^{k_2}\left(\Re\left(C_k^{\cdot}\frac{\partial C_k}{\partial b_{Lp}}\right)\right) = 0$$

(15)

where $\Re$ is Real.

The partial derivatives in (15) can be obtained as follows.

$$\frac{\partial C_k}{\partial a_{Lp}} = \frac{1}{N}\sum_{n=0}^{N-1}\left(\frac{\partial c_n}{\partial A_L}\frac{\partial A_L}{\partial a_{Lp}}\right)e^{-j\frac{2\pi kn}{N}}$$

$$\frac{\partial C_k}{\partial b_{Lp}} = \frac{1}{N}\sum_{n=0}^{N-1}\left(\frac{\partial c_n}{\partial \Phi_L}\frac{\partial \Phi_L}{\partial b_{Lp}}\right)e^{-j\frac{2\pi kn}{N}}$$

(16)

Since

$$\frac{\partial A_L}{\partial a_{Lp}} = (n\Delta t)^P$$

$$\frac{\partial \Phi_L}{\partial b_{Lp}} = (n\Delta t)^P$$

$$\frac{\partial c_n}{\partial A_L} = \frac{-x_n e^{j(2\pi L\ f_0\ n\ \Delta t+\phi_L)}}{\left(\sum_{m=-M}^{m=M} A_m e^{j(2\pi m\ f_0\ n\ \Delta t+\phi_m)}\right)^2}$$

$$\frac{\partial c_n}{\partial \Phi_L} = \frac{-x_n\left(jA_L e^{j(2\pi L\ f_0\ n\ \Delta t+\phi_L)}\right)}{\left(\sum_{m=-M}^{m=M} A_m e^{j(2\pi m\ f_0\ n\ \Delta t+\phi_m)}\right)^2}$$

(17)

then

$$\frac{\partial C_k}{\partial a_{Lp}} = \frac{1}{N}\sum_{n=0}^{N-1}\left(\frac{-x_n(n\Delta t)^P e^{j(2\pi L\ f_0\ n\ \Delta t+\phi_L)}}{\left(\sum_{m=-M}^{m=M} A_m e^{j(2\pi mf_0 n\Delta t+\phi_m)}\right)^2}\right)e^{-j\frac{2\pi kn}{N}}$$

$$\frac{\partial C_k}{\partial b_{Lp}} = \frac{1}{N}\sum_{n=0}^{N-1}\left(\frac{-jA_L x_n(n\Delta t)^P e^{j(2\pi L\ f_0\ n\ \Delta t+\phi_L)}}{\left(\sum_{m=-M}^{m=M} A_m e^{j(2\pi mf_0 n\Delta t+\phi_m)}\right)^2}\right)e^{-j\frac{2\pi kn}{N}}$$

(18)

6

where A_m and ϕ_m are functions of $n\Delta t$ for $m = -M, -(M-1), ..., -1, 1, 2 ..., M$. Note that the partial derivatives can be computed as DFTs of the time series inside the outermost brackets.

Solving (15) yields a set of $\{a_{mp}, b_{mp}, m = -M, -(M-1), ..., -1,1,2, ..., M$, and $p=0,1,2, ... \}$, which can be used in (4) to construct the solution set of $\{A_m, \phi_m, m = -M, -(M-1), ..., -1,1,2,..., M\}$. Substituting this solution set into (10) would result in $\{c_n, n=0, 1, 2, ... N-1\}$, a time series representing the composite signal of sea clutter, noise and possible targets.

3.0   Practical Implementation of the Optimization

The optimization process formulated in Section 2 is theoretically straightforward, but numerically complex. Difficulties exist in the numerical optimization because: (i) the number of harmonics (M) present in the signal is not known beforehand, and (ii) there is no assurance that the amplitudes and the fundamental frequency of the power line harmonics remains constant over a long period of time. A large value of M or a fluctuating power line frequency increases the number of parameters in the signal model, and thereby increases the numerical complexity of the process.

To simplify the process, one must use approximations in the signal model. There are two key factors involved in the model: the number of the harmonics and the stability of the harmonics. The number of the harmonics required depends on how the amplitude of the harmonic changes with the harmonic number. Generally the significance of the harmonic decreases rapidly with the absolute value of the harmonic number. Therefore the higher-order harmonics can be neglected. The stability of the interference harmonics depends on the stability of the amplitudes and the stability of the fundamental frequency. The amplitudes are normally stable with time. Therefore the constant term in the polynomial in (4) is likely to be adequate to approximate the amplitude. On the other hand, the frequency is determined in power generators, and it is likely to fluctuate. Therefore the higher-order terms may be required to approximate the frequency.

The higher-order terms for the frequency, however, increase the numerical complexity of the process tremendously. Further approximations are necessary to compromise for the simplicity of the process. Although the frequency fluctuates, it is expected to be very close to 60 Hz. In the following subsections, various assumptions are made in the model for the frequency: in Subsection 3.1, the frequency is assumed to be equal to the well-known value of 60 Hz, and then in Subsection 3.2, it is assumed to be equal to an unknown constant which may deviate slightly from 60 Hz. For each of the two assumptions, the process is simplified and the effectiveness of the process is investigated. Based on the results for the two cases, a revised approach to the optimization process is presented in Subsection 3.3.

3.1 Case of Constant Amplitudes and Constant Phases

3.1.1 Mathematical Simplification

The fundamental frequency of the harmonics in this case is constant at 60 Hz, and the signal model becomes

$$x_n = c_n \left(\sum_{m=-2}^{m=2} A_m e^{j(2\pi m \, f_0 \, n \, \Delta t + \phi_m)} \right) \tag{19}$$

where A_m and ϕ_m are constant.

The modulation replicas are now centred exactly at 5, 10, 15 and 20 Hz. At each of the centre frequencies, more than one modulation replica may exist due to multiple harmonic interference. These modulation replicas overlap each other, and they cannot be distinguished in the power spectrum. This implies that the modulation replicas caused by the higher-order harmonics ($m > 2$) appear to be the same as those caused by the lower-order harmonics ($m=+/-1$, $+/-2$). Therefore the higher-order harmonics can be ignored in the signal model.

The equations in (15) now become, for L=-2, -1, 1, 2,

$$\frac{\partial E}{\partial A_L} = \sum_{k=k_1}^{k_2} \left(\Re \left(C_k^* \frac{\partial C_k}{\partial A_L} \right) \right) = 0$$

$$\frac{\partial E}{\partial \Phi_L} = \sum_{k=k_1}^{k_2} \left(\Re \left(C_k^* \frac{\partial C_k}{\partial \Phi_L} \right) \right) = 0 \tag{20}$$

The partial derivatives of C_k in the equations are given by

$$\frac{\partial C_k}{\partial A_L} = \frac{1}{N} \sum_{n=0}^{N-1} \left(\frac{-x_n e^{j(2\pi L f_0 n \Delta t + \phi_L)}}{\left(\sum_{m=-2}^{m=2} A_m e^{j(2\pi m f_0 n \Delta t + \phi_m)} \right)^2} \right) e^{-j\frac{2\pi k n}{N}}$$

$$\frac{\partial C_k}{\partial \Phi_L} = \frac{1}{N} \sum_{n=0}^{N-1} \left(\frac{-j A_L x_n e^{j(2\pi L f_0 n \Delta t + \phi_L)}}{\left(\sum_{m=-2}^{m=2} A_m e^{j(2\pi m f_0 n \Delta t + \phi_m)} \right)^2} \right) e^{-j\frac{2\pi k n}{N}} \tag{21}$$

Note that since the amplitudes of the harmonics are assumed to be constant, the two partial derivatives can be related as

$$\frac{\partial C(k)}{\partial \Phi_L} = jA_L \frac{\partial C(k)}{\partial A_L}$$ (22)

This relationship can be used to simplify the second equation in (20), which then becomes

$$\sum_{k=k_1}^{k_2} \left(\Re\left(C_k^* \frac{\partial C_k}{\partial A_L} \right) \right) = 0$$

$$\sum_{k=k_1}^{k_2} \left(\Im\left(C_k^* \frac{\partial C_k}{\partial A_L} \right) \right) = 0$$ (23)

Where $\Im$ stands for Imaginary.

Solving (23) would yield a set of $\{A_m, \phi_m, m=-2, -1, 1, 2\}$, and substituting this set into (10) would result in $\{c_n, n=0, 1, 2, ... N-1\}$.

3.1.2 Numerical Implementation

In this simplified optimization process, there are still eight unknown variables. To efficiently implement this process, it is necessary to further reduce the number of the unknown variables. Since the Doppler spreads of the dominant sea clutter and the modulation spectral replicas are confined to narrow regions, they can be assumed to have very little interaction in the frequency domain. Each of the four interference peaks can therefore be optimized individually by selecting the appropriate range of Doppler frequency (i.e., k). For each of the interference peaks, there is only one interference harmonic, and therefore there are two unknown variables: the amplitude and the phase of the harmonic.

Instead of one optimization, however, four optimizations are now required. One is required for each of the four interference peaks. Furthermore, some iterations of the optimizations may be necessary. For the first iteration, the amplitudes and phases of the harmonics other than the one being optimized can be assumed to be zero. For the subsequent iterations, those amplitudes and phases can take the corresponding values found in the previous iteration.

3.1.3 Results and Discussions

This simplified process was first applied to some theoretical data. The data was generated exactly according to the signal model with a fundamental frequency of 60 Hz. As expected, this process completely suppressed the interference in the theoretical data.

The process was then applied to the experimental HFSWR time series in Figure 1. The result indicates that the process is ineffective. As shown in Figure 3, the peak power spectral density (PSD) is only slightly reduced at 10 and 15 Hz while the peak PSD is even increased at 5 and 20 Hz.

This poor performance indicates that the fundamental frequency of the harmonics is not exactly 60 Hz, and that there is a mismatch between the frequency in the model and the frequency in the data.

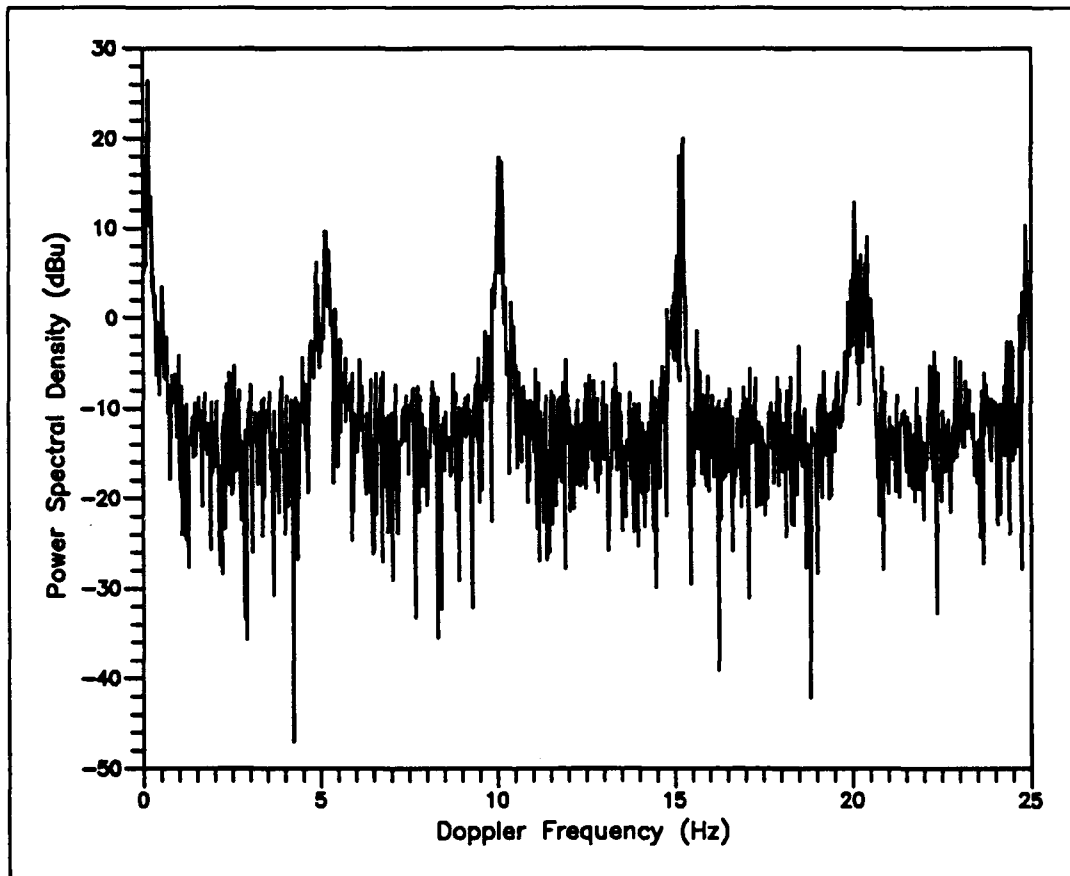Figure 2   Power Spectrum of the Experimental Time Series
                after Suppression of 60 Hz Harmonics

3.2   Case of Constant Amplitudes and Linear Phases

3.2.1   Mathematical Simplification

The fundamental frequency in the model for this case is still assumed to be constant. However, it may now deviate slightly from 60 Hz. A frequency offset, Δf, is introduced to indicate the deviation.

10

Since Δf is constant, the polynomials for the phases become linear. Based on the frequency multiplication assumption made earlier, the phase for the m-th harmonic becomes

$$\phi_m(n\ \Delta t) = b_{m0} + 2\pi(m\ \Delta f)N\ \Delta t \qquad (24)$$

Thus the signal model can be represented by

$$X_n = C_n\left(\sum_{m=-4}^{m=4} A_m e^{j(2\pi(mf_0)n\ \Delta t + 2\pi(m\Delta f)n\Delta t + b_m)}\right) \qquad (25)$$

where A_m and b_m are constants. Note that here we have dropped the subscript 0 in b_m, and we have also set M to be four.

The necessary conditions for minimizing the spectral power are:

$$\frac{\partial E}{\partial A_L} = \sum_{k=k_1}^{k_2}\left(\Re\left(C_k^*\frac{\partial C_k}{\partial A_L}\right)\right) = 0$$

$$\frac{\partial E}{\partial b_L} = \sum_{k=k_1}^{k_2}\left(\Re\left(C_k^*\frac{\partial C_k}{\partial b_L}\right)\right) = 0 \qquad (26)$$

for L=-4, -3, -2, -1, 1, 2, 3, 4, and

$$\frac{\partial E}{\partial(\Delta f)} = 2\sum_{k=k_1}^{k_2}\left(\Re\left(C_k^*\frac{\partial C_k}{\partial(\Delta f)}\right)\right) = 0 \qquad (27)$$

where

$$\frac{\partial C_k}{\partial A_L} = \frac{1}{N}\sum_{n=0}^{N-1}\left(\frac{-x_n e^{j(2\pi L(f_0+\Delta f)n\Delta t + b_L)}}{\left(\sum_{m=-4}^{m=4} A_m e^{j(2\pi m(f_0+\Delta f)n\Delta t + b_m)}\right)^2}\right)e^{-j\frac{2\pi kn}{N}}$$

$$\qquad (28)$$

$$\frac{\partial C_k}{\partial b_L} = \frac{1}{N}\sum_{n=0}^{N-1}\left(\frac{-jA_L x_n e^{j(2\pi L(f_0+\Delta f)n\Delta t + b_L)}}{\left(\sum_{m=-4}^{m=4} A_m e^{j(2\pi m(f_0+\Delta f)n\Delta t + b_m)}\right)^2}\right)e^{-j\frac{2\pi kn}{N}}$$

11

and

$$\frac{\partial C_k}{\partial(\Delta f)} = \frac{1}{N} \sum_{n=0}^{N-1} \left(\frac{-jA_L x_n (2\pi n\Delta t)\, e^{j(2\pi L(f_0+\Delta f)n\Delta t+b_L)}}{\left(\sum_{m=-4}^{m=4} A_m e^{j(2\pi m(f_0+\Delta f)n\Delta t+b_m)}\right)^2} \right) e^{-j\frac{2\pi kn}{N}} \tag{29}$$

Solving (26) and (27) would yield a set of $\{A_m, \phi_m, m=-4, -3, -2, -1, 1, 2, 3, 4\}$. Substituting this set into (10) would result in $\{c_n, n=0, 1, 2, ..., N-1\}$.

3.2.2   Numerical Implementation

Each of the interference peaks now consists of two harmonic modulation replicas. Therefore there are five unknown variables for the 60 Hz interference peak, and four unknown variables for the others. For each of the interference peaks, the variables include two amplitudes and two phases of the two harmonics. For the 60 Hz interference peak, the additional unknown variable is the frequency offset, Δf.

The implementation method of Subsection 3.1.2 can be used here. However, since the harmonics are periodic in this case, it may be difficult to locate the global minimum of the spectral power of the sea clutter. A different strategy for the numerical optimization is required. Our strategy involves a combination of optimizing and searching. For a given set of frequency offset and amplitudes of the two interference harmonics, we optimize the spectral power of the sea clutter with respect to the phases of the two harmonics. We then repeat the optimization for certain ranges of the frequency offset and the two amplitudes. Finally, we search for the frequency offset and the amplitudes of the two harmonics w ch would yield the global minimum.

3.2.3   Results and Discussions

This optimization process was also applied to the HFSWR time series shown in Figure 1. The frequency offset for this series was found to be -0.089 Hz. The power spectral density of the time series optimized by the process is shown in Figure 3. Although there is a significant improvement in the interference suppression, the process is still not very effective. Figure 3 shows that the peak PSD is reduced only by 3.5 dB at 5 Hz, 14.5 dB at 10 Hz, 11 dB at 15 Hz, and 6 dB at 20 Hz.

This result indicates that the fundamental frequency fluctuates and that the signal model with a constant frequency offset is still not quite adequate. This inadequacy is particularly severe in a long time series. To acquire a 1024-point time series at a PRF of 25 Hz, the radar must dwell for 40.96 Seconds. This is a very long duration as compared to the period of the 60 Hz interference. Consequently, the signal model with a constant frequency offset cannot adequately account for the fluctuation of the fundamental frequency.
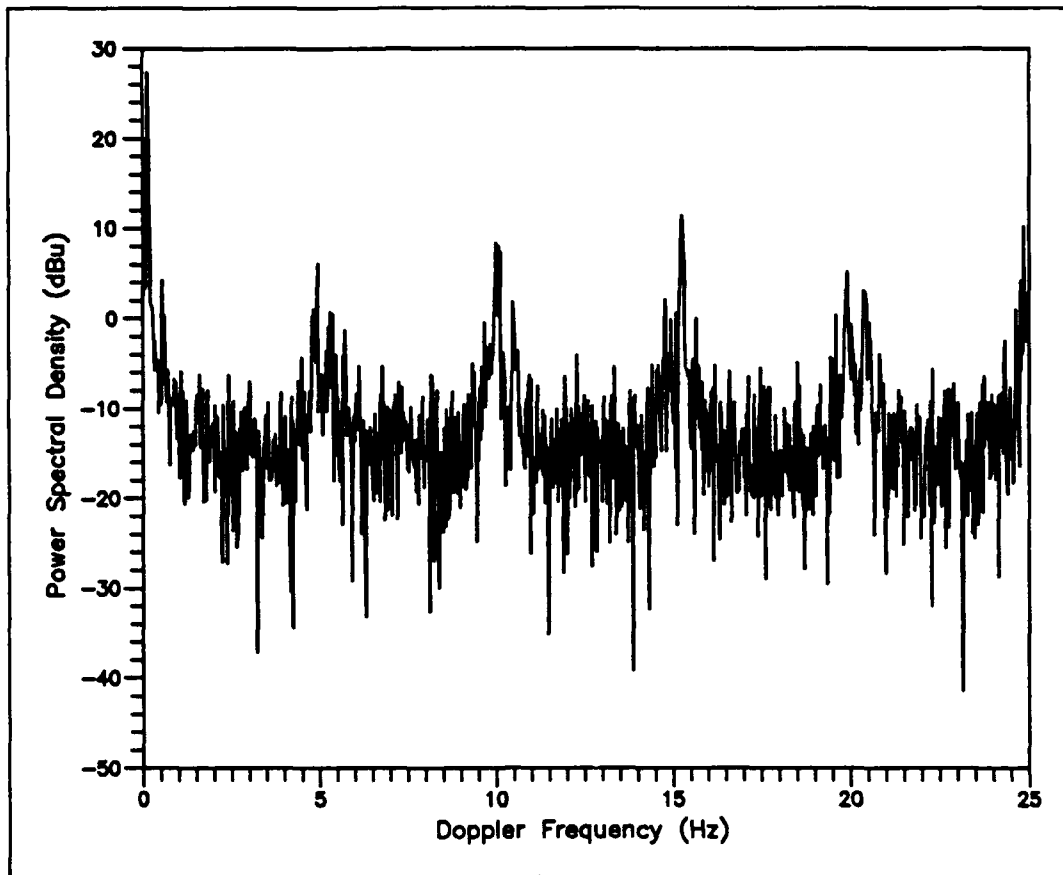
Figure 3   Power Spectrum of the Experimental Time Series
                  after Suppression of 59.911 Hz Harmonics

3.3   Case of Fluctuating Amplitudes and Fluctuating Phases

3.3.1   Short Time Series

The fluctuations of the amplitudes and the fundamental frequency, however, are expected to be very small in the HFSWR time series. For a short time series, the signal model of Subsection 3.2 should be more adequate to approximate the harmonics, and therefore, the optimization process should work more effectively.

Figure 4 shows the PSD of a 256-point HFSWR time series before and after the optimization. The interference is suppressed substantially in this short time series. The peak PSD is reduced by more than 10 dB near 5 and 20 Hz, and more than 20 dB near 10 and 15 Hz.

Figure 4 also shows that the optimization process satisfies the requirement that the noise and sea-clutter statistics must be preserved in the time series. The power spectrum is virtually unchanged in the non-interfered frequency regions before and after the optimization.
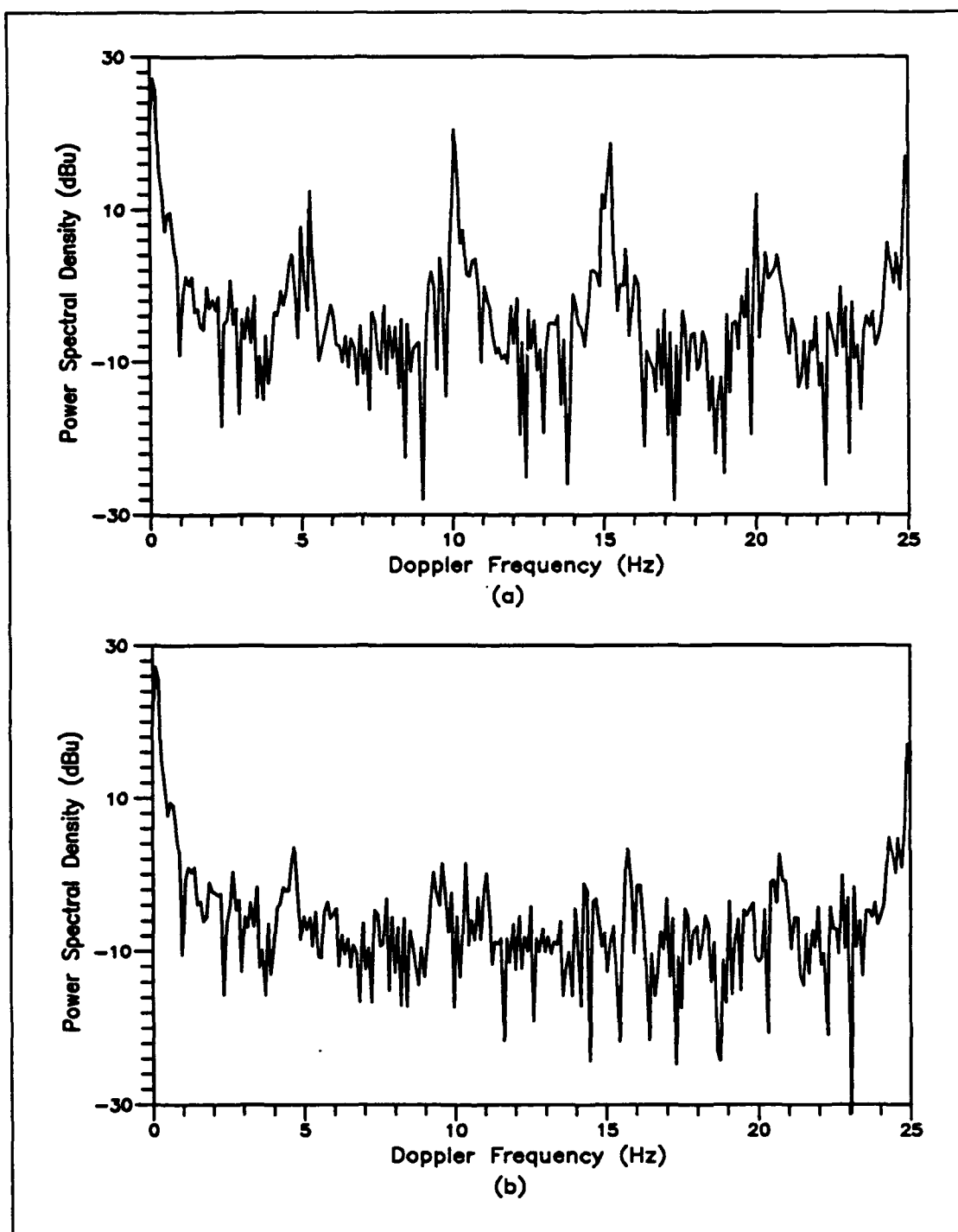
13

Figure 4   Power Spectrum of a 256-Point HFSWR Time Series
            before (a) and after (b) Suppression of 59.947 Hz Harmonics

14

3.3.2 Long Time Series

The result for the short time series indicates that an alternate approach can be used for the long time series. The long series can be divided into several short series, and the short series can be optimized individually by the process of Subsection 3.2. After the optimizations, the short series can then be grouped back together.

This approach was also applied to the HFSWR time series shown in Figure 1. The 1024-point time series was divided into 8 segments of 128 points, and each of the 8 data segments was then optimized with the process of Subsection 3.2. The optimized data segments were finally assembled together to form a new series. Figure 5 shows the PSD of the time series after the optimizations. The result indicates that this new approach is much more effective. Substantial suppression of the interference is now achieved in the time series. The peak PSD of the time series is reduced respectively by 13 dB at 5 Hz, 22 dB at 10 Hz, 15 dB at 15 Hz, and 14 dB at 20 Hz.

Figure 5 indicates that the optimizations not only preserve the shape of the power spectrum in the non-interfered frequency regions, but also try to restore the noise level in the time series. In the original time series, the noise level has been raised because of the interference. After the interference suppression, the PSD level of the time series is noticeably reduced.
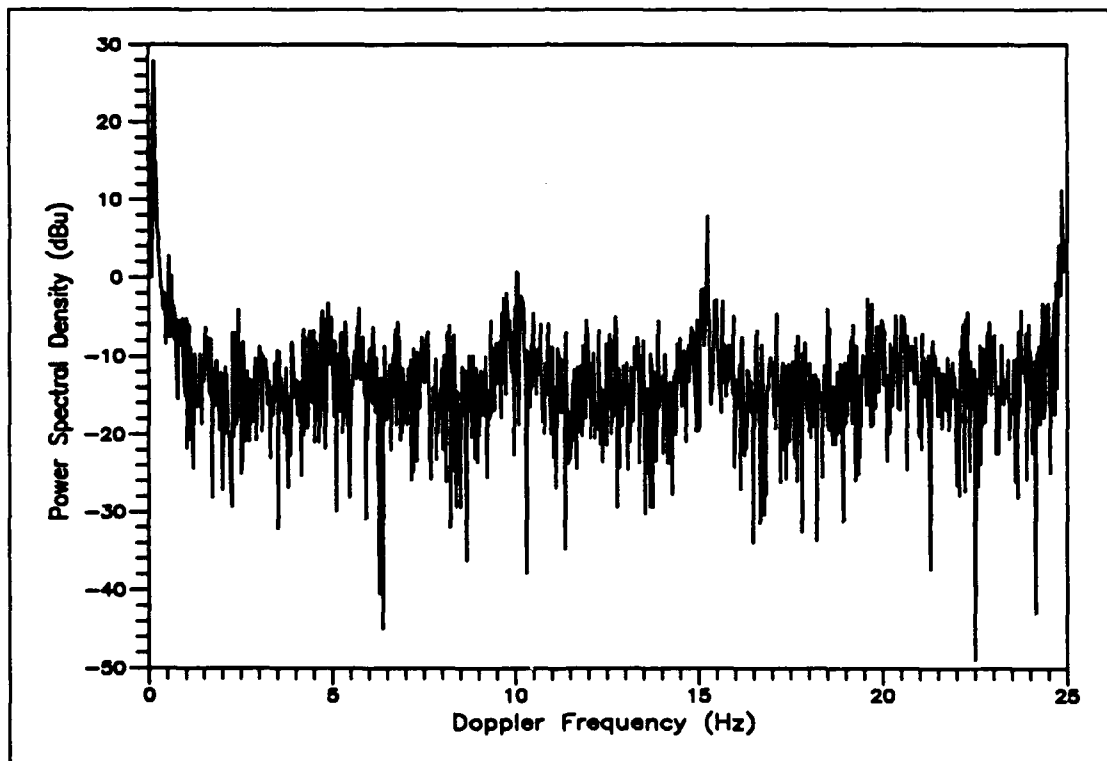

Figure 5   Power Spectrum of the Experimental Time Series
after Interference Suppression in Individual Segments

15

The PSD reductions at 5 and 20 Hz are particularly significant because the radar target signals normally appear in the low Doppler frequency region, i.e., in the regions between 0 and 5 Hz, and between 20 and 25 Hz. Severe interference may mask out the target signals in these regions.

A small degree of interference, however, remains in the optimized time series in Figure 5. This residual interference is due to the fact that the signal model is only an approximation to the fluctuating harmonics.

3.4 Anomalies in HFSWR Data

The effectiveness of the optimization process also depends on the quality of the HFSWR data. Sometimes the HFSWR data contains anomalies. Figure 6 depicts a 4096-point HFSWR time series before and after the application of the optimization process. In the original time series, there is a large noise spike near 75 seconds. Following the 75 second mark, the interference in the I and Q channels appear peculiarly of unequal strength. Our optimization process does not account for these anomalies. Consequently, they may have some negative effects on the optimization results. The time series in Figure 6 was optimized with the revised approach of Subsection 3.3.2. The original 4096-point time series was divided into 16 data segments of 256 points, and each of the segments was optimized with the process of Subsection 3.2. The results indicate that the process works effectively for the data segments before the 75 second mark. In fact, the 256-point time series shown in Figure 4 is the first segment of this 4096-point series, and a substantial reduction of the interference was achieved for the segment. However, the process works much less effectively for the data segments after the 75 second mark, and a large amount of interference remains in the data segments after the optimizations. In the last three 256-point data segments in particular, the process fails to construct a good waveform in the Q channel.

The remaining interference in the segments after the 75 second mark contributes significantly to the residual interference in the long time series. Figure 7 shows the power spectrum of the 4096-point time series before and after the optimizations. The peak PSD of the series is reduced by more than 15 dB near 10 and 15 Hz, and more than 5 dB near 5 and 20 Hz. However, it is evident that there is still some interference remaining in the optimized time series.
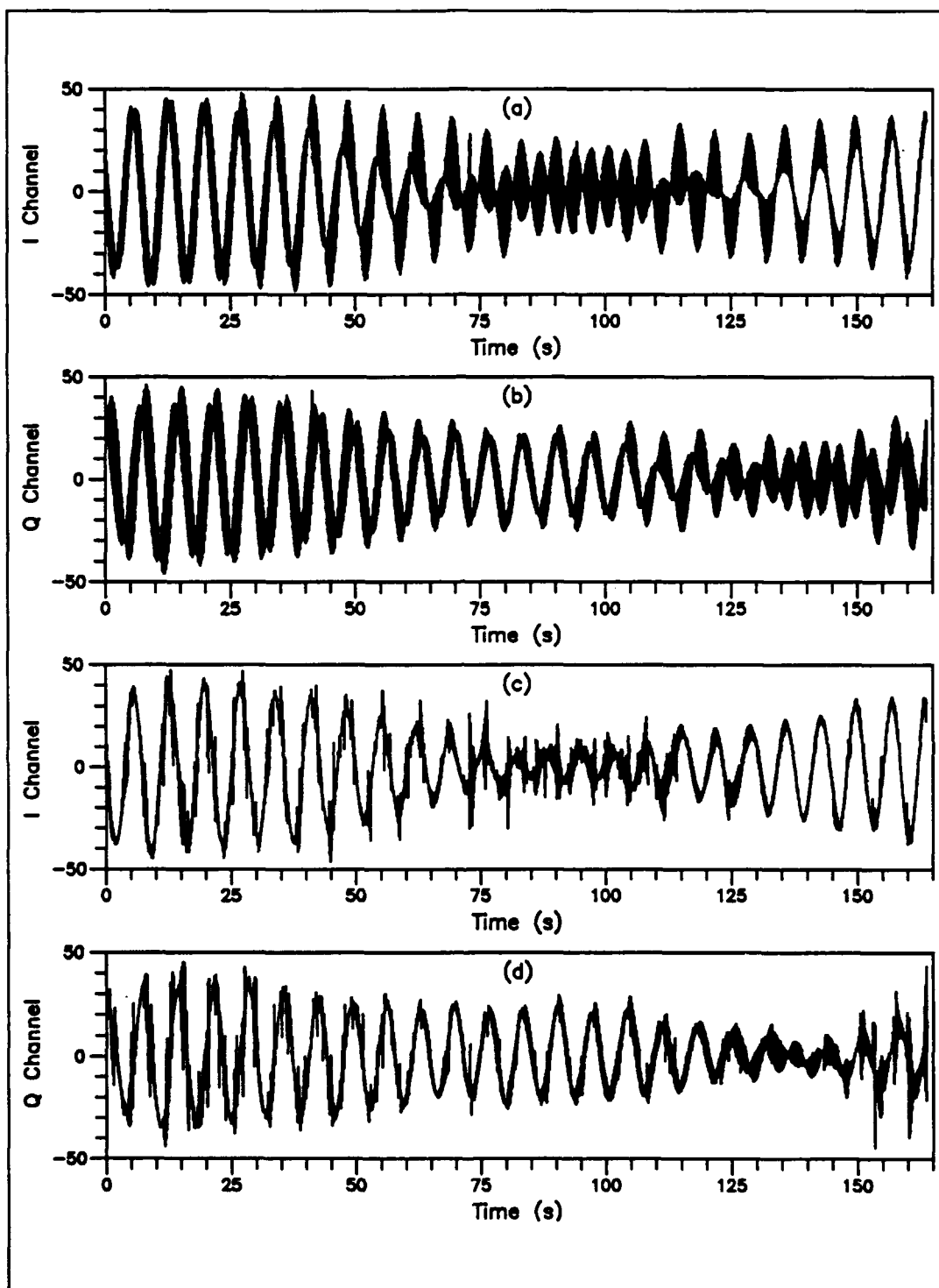
16

Figure 6   I and Q Channels of a 4096-point HFSWR Time Series
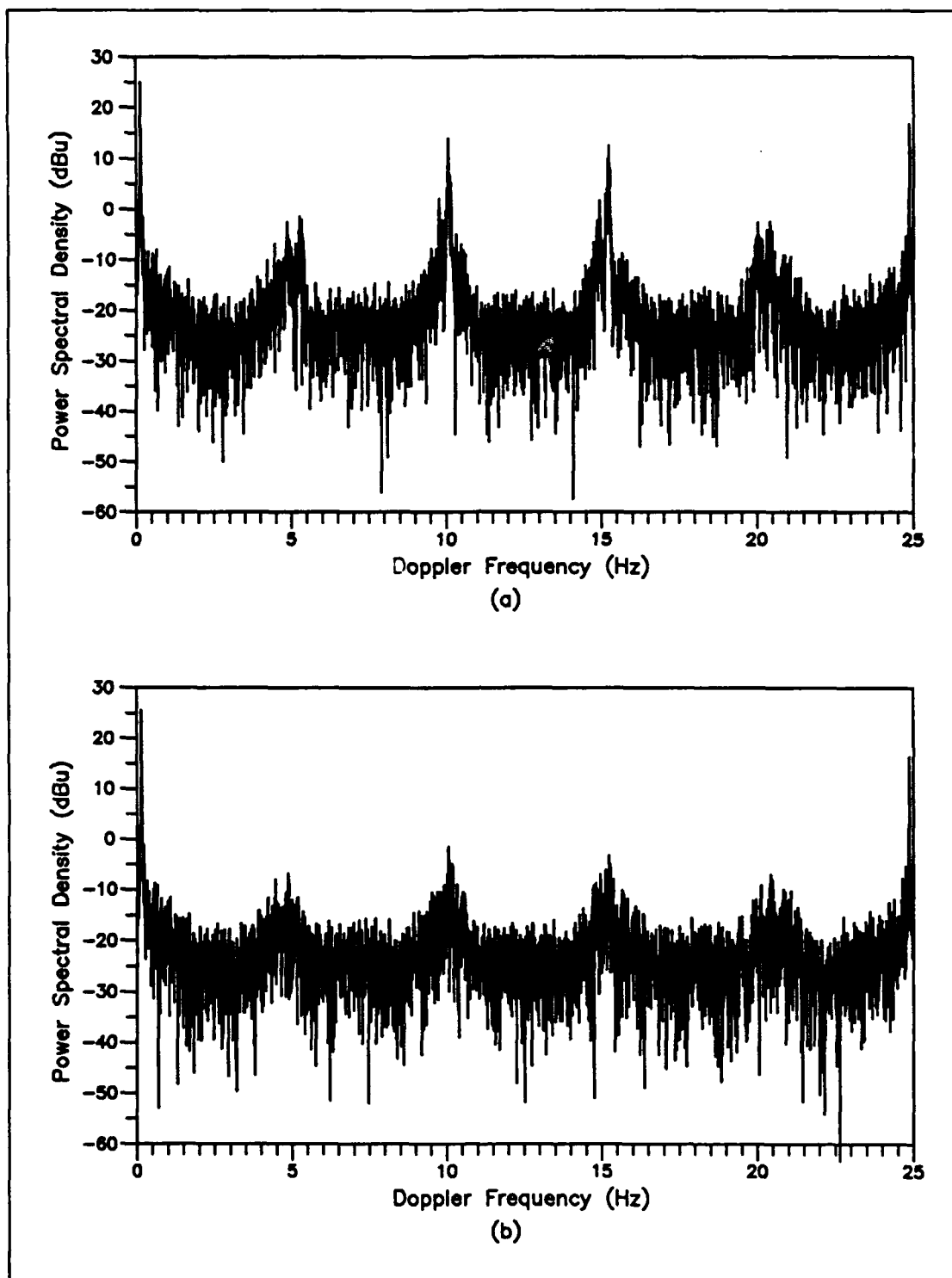   before (a,b) and after (c,d) Interference Suppression

17

Figure 7   Power Spectrum of the 4096-point HFSWR Time Series
before (a) and after (b) Interference Suppression

Figure 6 also indicates that there are some noise spikes in the optimized time series. These spikes are probably caused by an irregular waveform pattern in the original time series. The original time series was under-sampled, and therefore the time waveform of the series would appear to be flat at one instance and spiking at the others. These flat and spiking regions would normally appear in a very regular pattern. However, in the experimental time series, this regular pattern does not always exist. For instance, in Figure 8(a), where a magnified portion of the Q channel in Figure 6 is shown, irregular patterns occur in the small intervals near 1 and 5 seconds. A close examination of the time series indicates that the noise spikes in the optimized time series appear exactly in the same regions where the irregular waveform patterns appear in the original time series. This concurrent occurrence of the irregular waveform patterns and the noise spikes is illustrated in Figure 8(b), where the Q channel of the time series is further magnified before and after the optimization.
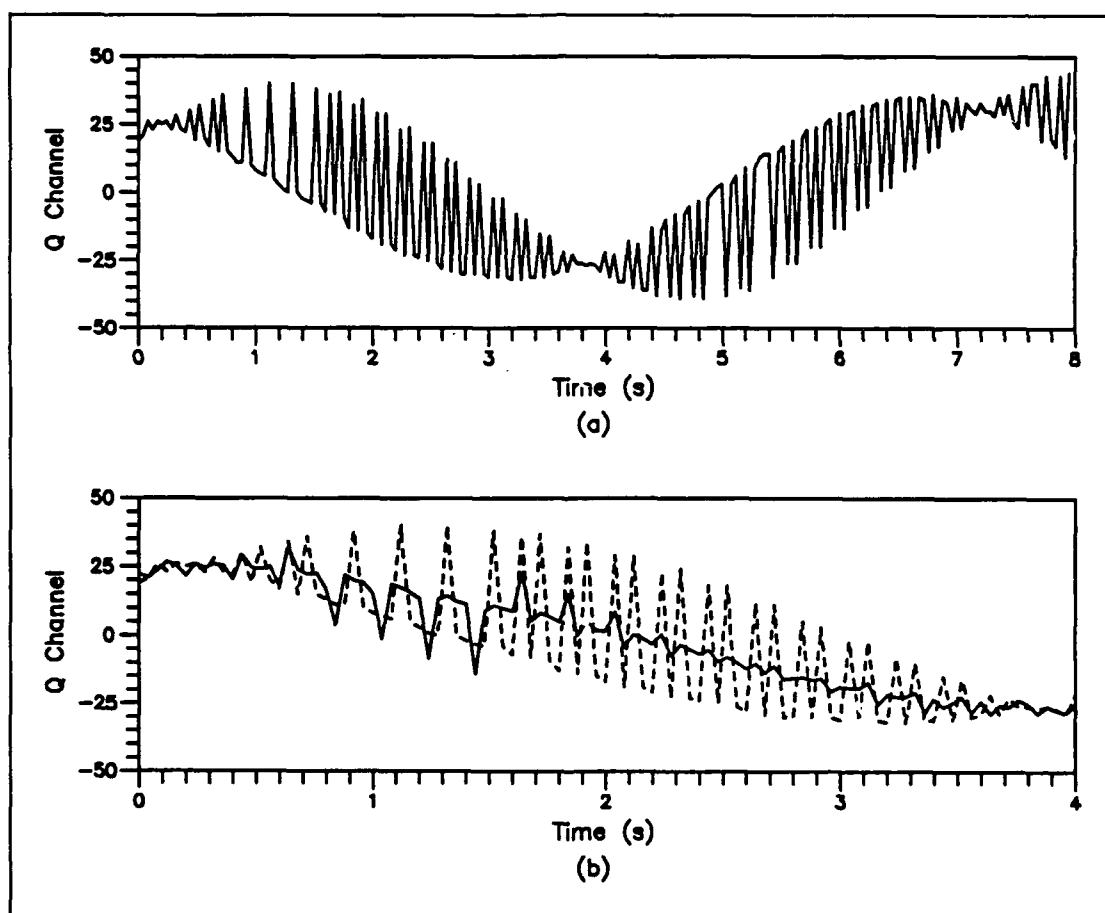

Figure 8   Irregular Waveform Patterns and Noise Spikes
(a) Q Channel;
(b) Q Channel before (dashed) and after (solid) Optimization

19

3.5 Summary

The results in Section 3 can be summarized below:

(1) To avoid numerical complexities, one must use approximations in the signal model for the fluctuating amplitudes and fundamental frequency of the interference harmonics.

(2) If the amplitudes and the fundamental frequency of the harmonics are approximated with constants, the optimization process works more effectively for a short time series than for a long time series. Substantial reductions of the interference can be achieved in the short HFSWR time series. More than 20 dB suppression of the peak interference PSD is possible in some 256-point time series.

(3) The result for the short time series leads to a different approach for the long time series. The long series is divided into several short series and each of the short series is optimized individually. With this revised approach, it is possible to reduce substantially the spectral power of interference. Up to 20 dB reduction of the peak interference can be achieved in a 1024-point HFSWR time series.

(4) The optimization process, however, becomes less effective if anomalies exist in the experimental time series. The possible anomalies include (i) large noise spikes, (ii) unequal strengths of interference in I and Q channels, and (iii) irregular patterns in the time waveform.

4.0 Conclusions and Recommendations

4.1 Conclusions

The need for noise and sea clutter statistics in the contaminated HFSWR data leads to the formulation of an optimization process. This process has the capability of suppressing the interference of power line harmonics without adversely altering the noise and sea-clutter statistics in the data.

The process, however, relies on adequate modelling of the power line harmonics. The harmonics may have a fluctuating fundamental frequency and time-dependent amplitudes. A large number of parameters are required in the signal model. Consequently, the process can be numerically complex.

To implement our process, one must use approximations in the signal model. For short time series, the amplitudes and the fundamental frequency of the harmonics can be approximated with constants, and the process can still be effective. For some 256-point time series, more than 20 dB reduction of the peak interference PSD is possible. For a long HFSWR time series, the same process can be applied by first dividing it into several short data segments (e.g., 256 points or even 128 points), and then optimizing in the individual data segments. With this revised approach, up to 20 dB of the peak interference can be suppressed for a long HFSWR time series.

The optimization process, however, becomes less effective if the experimental HFSWR time series contains anomalies. The possible anomalies include (i) large noise spikes, (ii) unequal strengths of interference in I and Q channels, and (iii) irregular patterns in the waveform of the time series.

4.2   Recommendations

Although the optimization process substantially reduces the interference, a small degree of the interference still remains in the optimized time series. This residual interference is partly due to the approximations used in the signal model for the fluctuating fundamental frequency of the harmonics.

A better approximation for the fundamental frequency can be obtained in the processing of the raw radar data [3]. If this approximation is used, the optimization process should be able to reduce the interference more substantially.

Acknowledgement

Suggestions provided by Dr. H.C. Chan are gratefully acknowledged.

References

1.   A. M. Ponsford and S. K. Srivastava, "Groundwave Radar Development at NORDCO Limited", Interim Report to DND, March 1,1990.

2.   A. V. Oppenheim and R. W. Schafer, "Digital Signal Processing", p.28, Prentice-Hall, Inc, New Jersey, 1975.

3.   H. C. Chan, "Development of Software and Preliminary Analysis of High-Frequency Surface Wave Radar Data", DREO Report (under internal review), Defence Research Establishment Ottawa.

Appendix A Characteristics of the Spectral Power Function

Figure A-1 depicts the spectral power of interference against the frequency offset and amplitudes of two different harmonics (60 and -240 Hz) producing the same interference peak. The frequency offset ranges from -0.10 to -0.01 Hz while the amplitudes range from 0.25 to 0.45 for the 60 Hz harmonic and from 0 to 0.05 for the -240 Hz harmonic. For a given set of the frequency offset and the two amplitudes, the spectral power was optimized by the process of Subsection 3.2 with respect to the phases of the two harmonics in a 256-point data series. Each point (a cross) in the plot represents an optimization. This plot shows that there is indeed an global minimum for this spectral power function.

Figure A-1 also shows that the spectral power function is very sensitive to the fluctuation of the fundamental frequency of the harmonic interference. Near its minimum, the spectral power does not change very much with different combinations of the two amplitudes. However, it changes rapidly with the frequency offset.
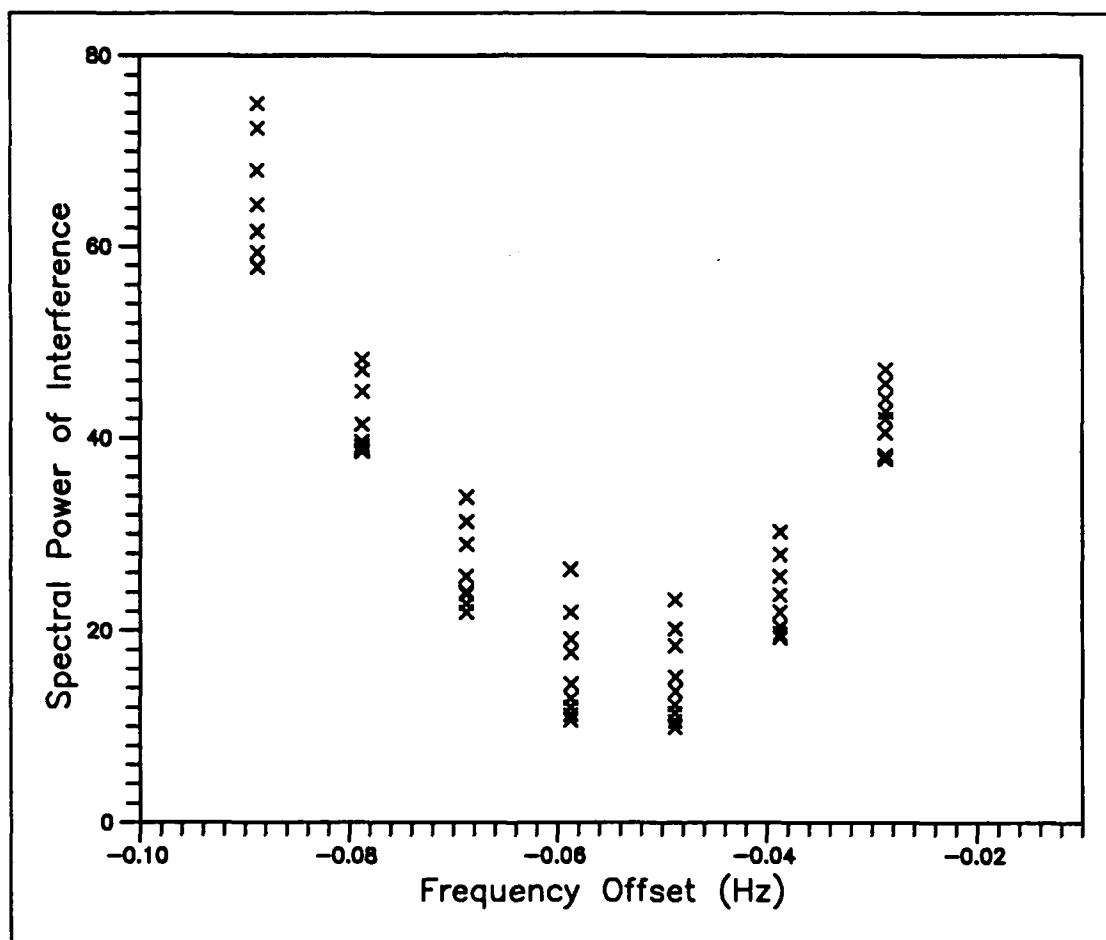

Figure A-1 Spectral Power of Interference vs. Amplitudes and Frequency

SECURITY CLASSIFICATION OF FORM
(highest classification of Title, Abstract, Keywords)

-23-

DOCUMENT CONTROL DATA

(Security classification of title, body of abstract and indexing annotation must be entered when the overall document is classified)

1. ORIGINATOR (the name and address of the organization preparing the document. Organizations for whom the document was prepared, e.g. Establishment sponsoring a contractor's report, or tasking agency, are entered in section 8.) DEFENCE RESEARCH ESTABLISHMENT OTTAWA 3701 CARLING AVENUE, OTTAWA, ONTARIO, K1A 0Z4	2. SECURITY CLASSIFICATION (overall security classification of the document. including special warning terms if applicable) UNCLASSIFIED

3. TITLE (the complete document title as indicated on the title page. Its classification should be indicated by the appropriate abbreviation (S.C or U) in parentheses after the title.)

SUPPRESSION OF POWER LINE HARMONIC INTERFERENCE
IN HF SURFACE-WAVE RADAR (U)

4. AUTHORS (Last name, first name, middle initial)

LEONG, HANK W. H.

5. DATE OF PUBLICATION (month and year of publication of document) OCTOBER, 1992	6a. NO. OF PAGES (total containing information. Include Annexes, Appendices, etc.) 22	6b. NO. OF REFS (total cited in document) 3

7. DESCRIPTIVE NOTES (the category of the document, e.g. technical report, technical note or memorandum. If appropriate, enter the type of report, e.g. interim, progress, summary, annual or final. Give the inclusive dates when a specific reporting period is covered.)

TECHNICAL REPORT

8. SPONSORING ACTIVITY (the name of the department project office or laboratory sponsoring the research and development. Include the address.)
DEFENCE RESEARCH ESTABLISHMENT OTTAWA
3701 CARLING AVENUE, OTTAWA, ONTARIO, K1A 0Z4

9a. PROJECT OR GRANT NO. (if appropriate, the applicable research and development project or grant number under which the document was written. Please specify whether project or grant) 041LR	9b. CONTRACT NO. (if appropriate, the applicable number under which the document was written)
10a. ORIGINATOR'S DOCUMENT NUMBER (the official document number by which the document is identified by the originating activity. This number must be unique to this document.) DREO REPORT No. 1137	10b. OTHER DOCUMENT NOS. (Any other numbers which may be assigned this document either by the originator or by the sponsor)

11. DOCUMENT AVAILABILITY (any limitations on further dissemination of the document, other than those imposed by security classification)

(X) Unlimited distribution
( ) Distribution limited to defence departments and defence contractors; further distribution only as approved
( ) Distribution limited to defence departments and Canadian defence contractors; further distribution only as approved
( ) Distribution limited to government departments and agencies; further distribution only as approved
( ) Distribution limited to defence departments; further distribution only as approved
( ) Other (please specify):

12. DOCUMENT ANNOUNCEMENT (any limitation to the bibliographic announcement of this document. This will normally correspond to the Document Availabilty (11). However, where further distribution (beyond the audience specified in 11) is possible, a wider announcement audience may be selected.)

UNLIMITED

13. ABSTRACT (a brief and factual summary of the document. It may also appear elsewhere in the body of the document itself. It is highly desirable that the abstract of classified documents be unclassified. Each paragraph of the abstract shall begin with an indication of the security classification of the information in the paragraph (unless the document itself is unclassified) represented as (S), (C), or (U). It is not necessary to include here abstracts in both offical languages unless the text is bilingual).

Experimental data of the Cape Bonavista High-Frequency Surface-Wave Radar (HFSWR) facility was contaminated by power line harmonics. The harmonics modulate the radar signal (mainly sea clutter) and replicate it into the Doppler spectrum. The spectral replicas distort the noise and sea clutter statistics in the signal. It is necessary to suppress them before the statistics can be obtained.

A new process based on optimizations is presented for suppressing the interference. This process minimizes the spectral power of the sea clutter with respect to the amplitudes and phases of the harmonics. It is capable of removing the spectral replicas without adversely altering the statistics. This process, however, requires adequate modelling of the harmonics. A large number of parameters are required because the harmonics may have a fluctuating fundamental frequency and fluctuating amplitudes. Therefore the process can be numerically complex. To implement our process, one must use approximations in the signal model. If the amplitudes and the fundamental frequency are approximated with constants, the process can still be effective for a short HFSWR data series. For some 256-point data series, more than 20 dB of the peak interference can be reduced. For a long HFSWR data series, the same process can be applied by first dividing it into several short data segments, and then optimizing on the individual segments. With this slightly revised approach, up to 20 dB of the peak interference can be suppressed for a long data series.

The process does not account for any anomalies in the HFSWR data. The data may sometimes have (i) large noise spikes, (ii) unequal strengths of interference in I and Q channels, and (iii) irregular waveform patterns. If these anomalies exist, the process becomes less effective.

14. KEYWORDS, DESCRIPTORS or IDENTIFIERS (technically meaningful terms or short phrases that characterize a document and could be helpful in cataloguing the document. They should be selected so that no security classification is required. Identifiers, such as equioment model designation, trade name, military project code name, geographic location may also be included. If possible keywords should be selected from a published thesaurus. e.g. Thesaurus of Engineering and Scientific Terms (TEST) and that thesaurus-identified. If it is not possible to select indexing terms which are Unclassified, the classification of each should be indicated as with the title.)

RADAR, RADAR SIGNAL, POWER LINE HARMONIC INTERFERENCE, INTERFERENCE SUPPRESSION, OPTIMIZATION